

Centrality dependence of charged hadron transverse momentum spectra in d+Au collisions at $\sqrt{s_{NN}} = 200$ GeV

B.B.Back¹, M.D.Baker², M.Ballintijn⁴, D.S.Barton², B.Becker², R.R.Betts⁶, A.A.Bickley⁷, R.Bindel⁷, A.Budzanowski³, W.Busza⁴, A.Carroll², M.P.Decowski⁴, E.García⁶, T.Gburek³, N.George^{1,2}, K.Gulbrandsen⁴, S.Gushue², C.Halliwell⁶, J.Hamblen⁸, A.S.Harrington⁸, C.Henderson⁴, D.J.Hofman⁶, R.S.Hollis⁶, R.Hołyński³, B.Holzman², A.Iordanova⁶, E.Johnson⁸, J.L.Kane⁴, N.Khan⁸, P.Kulinich⁴, C.M.Kuo⁵, J.W.Lee⁴, W.T.Lin⁵, S.Manly⁸, A.C.Mignerey⁷, A.Noell⁷, R.Nouicer^{2,6}, A.Olszewski³, R.Pak², I.C.Park⁸, H.Pernegger⁴, C.Reed⁴, L.P.Remsberg², C.Roland⁴, G.Roland⁴, J.Sagerer⁶, P.Sarin⁴, P.Sawicki³, I.Sedykh², W.Skulski⁸, C.E.Smith⁶, P.Steinberg², G.S.F.Stephans⁴, A.Sukhanov², R.Teng⁸, M.B.Tonjes⁷, A.Trzupek³, C.Vale⁴, G.J.van Nieuwenhuizen⁴, R.Verdier⁴, G.I.Veres⁴, B.Wadsworth⁴, F.L.H.Wolfs⁸, B.Wosiek³, K.Woźniak³, A.H.Wuosmaa¹, B.Wysłouch⁴, J.Zhang⁴

(PHOBOS Collaboration)

¹ Argonne National Laboratory, Argonne, IL 60439-4843, USA

² Brookhaven National Laboratory, Upton, NY 11973-5000, USA

³ Institute of Nuclear Physics, Kraków, Poland

⁴ Massachusetts Institute of Technology, Cambridge, MA 02139-4307, USA

⁵ National Central University, Chung-Li, Taiwan

⁶ University of Illinois at Chicago, Chicago, IL 60607-7059, USA

⁷ University of Maryland, College Park, MD 20742, USA

⁸ University of Rochester, Rochester, NY 14627, USA

(Dated: November 4, 2018)

We have measured transverse momentum distributions of charged hadrons produced in d+Au collisions at $\sqrt{s_{NN}} = 200$ GeV. The spectra were obtained for transverse momenta $0.25 < p_T < 6.0$ GeV/c, in a pseudorapidity range of $0.2 < \eta < 1.4$ in the deuteron direction. The evolution of the spectra with collision centrality is presented in comparison to $p + \bar{p}$ collisions at the same collision energy. With increasing centrality, the yield at high transverse momenta increases more rapidly than the overall particle density, leading to a strong modification of the spectral shape. This change in spectral shape is qualitatively different from observations in Au+Au collisions at the same energy. The results provide important information for discriminating between different models for the suppression of high- p_T hadrons observed in Au+Au collisions.

PACS numbers: 25.75.-q, 25.75.Dw, 25.75.Gz

The yield of charged hadrons produced in collisions of deuterons with gold nuclei at an energy of $\sqrt{s_{NN}} = 200$ GeV has been measured with the PHOBOS detector at the Relativistic Heavy Ion Collider (RHIC) at Brookhaven National Laboratory. The data are presented as a function of transverse momentum (p_T) and collision centrality. The goal of these measurements is to study the modification of particle production due to initial state effects in the nuclear medium, in comparison to nucleon-nucleon collisions at the same energy. Measurements from proton-nucleus (p+A) reactions at lower collision energies have found that the cross-section for hadron production at p_T of 1.5 to 5 GeV/c rises faster than the nuclear size A [1]. This observation, which is commonly called the Cronin effect, has been described as the result of initial state multiple scattering, leading to a broadening of the p_T distribution [2].

The present interest in repeating these measurements

at higher energies is motivated by results from Au+Au collisions at $\sqrt{s_{NN}} = 130$ and 200 GeV. In these collisions, the expected scaling of hadron production with the number of binary nucleon-nucleon collisions at p_T of 2–10 GeV/c is strongly violated [3, 4, 5, 6]. This effect had been predicted as a consequence of the energy loss of high- p_T partons in the hot and dense medium formed in Au+Au collisions [7]. The interpretation of the Au+Au data relies on the understanding of initial state effects, including gluon saturation [8], which can be investigated with the d+Au data presented here [9]. Similar measurements are reported in [10, 11]. By studying the spectra as a function of collision centrality, we can control the effective thickness of nuclear matter traversed by the incoming partons.

The data were collected using the PHOBOS two-arm magnetic spectrometer [12]. The spectrometer arms are each equipped with 16 layers of silicon sensors, providing

charged particle tracking both outside and inside the 2 T field of the PHOBOS magnet. Additional silicon detectors used in this analysis are the central single-layer Octagon barrel detector and the three single-layer forward Ring detectors located on either side of the interaction point.

The primary event trigger (Level 0) was provided by two sets of 16 scintillator counters (“Paddle counters”) covering pseudorapidities $3 < |\eta| < 4.5$. In addition, two higher level trigger conditions were used. Collisions close to the nominal vertex position $z_{vtx} = 0$ along the longitudinal (z) direction were selected using the time difference between signals in two rings of ten Čerenkov counters. The counters covered $-4.9 < \eta < -4.4$ and $3.6 < \eta < 4.1$, respectively. For part of the data set, a further online selection of events was accomplished using two arrays of horizontally segmented scintillator hodoscopes. One array was positioned immediately behind the spectrometer and the other at a distance of ~ 5 m from the interaction point. In combination with the known vertex position, a spatial coincidence from the hodoscopes was used to trigger on high- p_T particles which traverse the spectrometer.

Previous measurements of p+A collisions have shown a strong dependence of the multiplicities and momentum distributions of produced particles on the size of the target nucleus [1, 13]. For d+Au collisions, this implies the importance of characterizing the collision centrality. For a given event selection, the centrality can be quantified by a number of variables such as the average number of participating nucleons $\langle N_{part} \rangle$ or the average number of binary nucleon-nucleon collisions, $\langle N_{coll} \rangle$. Neither of these variables can be directly measured. Estimates of $\langle N_{part} \rangle$ or $\langle N_{coll} \rangle$ for a given event selection are typically obtained by matching the distribution of an experimental observable, such as the multiplicity in a certain η -region, with the results of a Glauber model calculation and detector simulation [14].

Centrality Selection	$\langle N_{part} \rangle$	$\langle N_{coll} \rangle$	Efficiency
0–20%	15.5 ± 1.0	14.6 ± 0.9	82%
20–40%	10.9 ± 0.9	9.7 ± 0.8	73%
40–70%	6.7 ± 0.9	5.4 ± 0.8	49%
70–100%	3.3 ± 0.7	2.2 ± 0.6	14%

TABLE I: Estimated values for $\langle N_{part} \rangle$ and $\langle N_{coll} \rangle$ and the respective systematic uncertainties for the four centrality bins used in this analysis. Also shown is the average event selection efficiency for each of the bins. The centrality bins are based on the signal of multiplicity counters covering $3.0 < |\eta| < 5.4$.

The centrality cuts for this analysis were based on the signal (E_{Ring}) of the three Ring detectors in the region of $3.0 < |\eta| < 5.4$, which is proportional to the

number of charged particles hitting these counters. In the MC simulations, centrality cuts on E_{Ring} were found to introduce a bias on the yield in the spectrometer acceptance of less than 5% for $\langle N_{part} \rangle > 3$, compared to cutting directly on N_{part} . If the N_{part} determination is based on a multiplicity region closer to the spectrometer acceptance, MC studies, as well as our data, showed a significantly larger bias at low and high centralities. For each of the four bins in E_{Ring} , $\langle N_{part} \rangle$ and $\langle N_{coll} \rangle$ were obtained from a Glauber model calculation using HIJING [15] and a full detector simulation which included the experimental trigger and event selection efficiency. In the HIJING calculations, the default value for the inelastic nucleon-nucleon cross-section of 41 mb was used, consistent with previous calculations [14].

The resulting estimates for $\langle N_{part} \rangle$ and $\langle N_{coll} \rangle$ in the four E_{Ring} -based centrality bins are shown in Table I. The percentage numbers refer to the fractional cross-section in the unbiased HIJING distribution. The determination of $\langle N_{part} \rangle$ and $\langle N_{coll} \rangle$ takes into account the bias introduced in the centrality by the online and offline event selection in the relatively low-multiplicity d+Au events. The largest contribution to this bias comes from the online vertex trigger, leading to the average event selection efficiencies for the individual centrality bins shown in Table I.

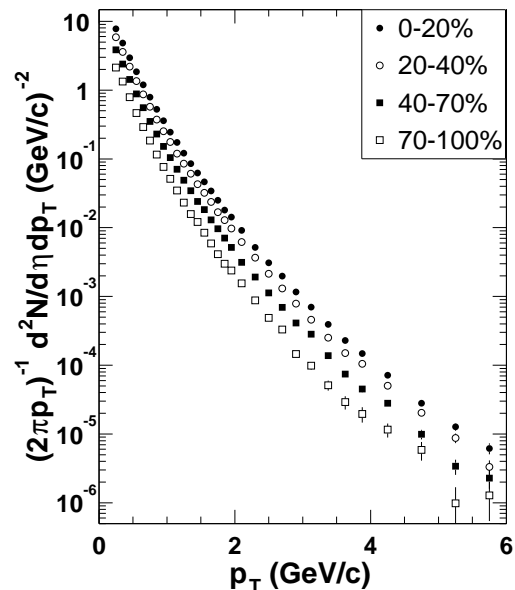


FIG. 1: Invariant yield of charged hadrons, $\frac{h^+ + h^-}{2}$, as a function of p_T for four centrality bins. Only statistical errors are shown.

Details of the track reconstruction algorithm can be found in [6, 16]. To optimize the momentum resolution

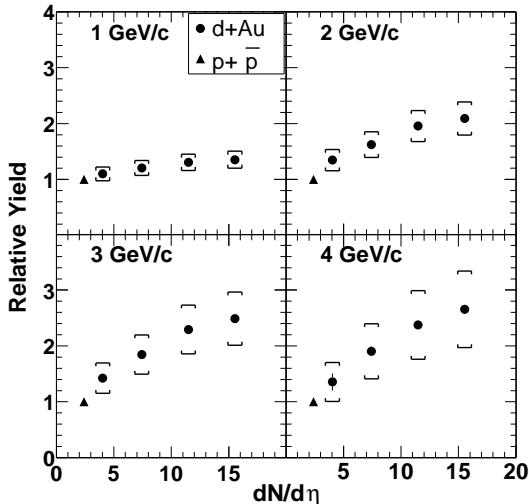


FIG. 2: The relative yield of d+Au to UA1 $p+\bar{p}$ data at $p_T = 1, 2, 3$ and 4 GeV/c is shown as a function of the integrated yield $dN/d\eta$ for the four E_{Ring} centrality bins. The ratio d+Au/ $p+\bar{p}$ has been normalized to unity at $p_T = 0.5$ GeV/c. The triangles indicate the values for $p+\bar{p}$. The brackets indicate the systematic errors on the relative yield (90% C.L.). The systematic error on $dN/d\eta$ is 12%.

and minimize systematic errors in the track selection, only particles traversing the full spectrometer arms were included in the analysis. These particles leave a minimum of 12 hits in the silicon detectors. This selection limits the usable vertex range to $-15 \text{ cm} < z_{vtx} < +10 \text{ cm}$. Due to the low multiplicity in d+Au collisions, a new algorithm for the offline determination of the collision vertex was developed, using hit position and energy information in the Octagon detector. MC studies show a resolution in the beam direction of $\sigma_{vtx_z} = 1.4 \text{ cm}$ for the most peripheral events and $\sigma_{vtx_z} = 0.8 \text{ cm}$ for the most central events. The transverse position of the event vertex was centered at the known position of the beam orbit. Unlike in the Au+Au track finding, the vertex position information was not included in the initial track seed.

To obtain the invariant yield of charged hadrons, we accumulated equal amounts of data with both magnet polarities. The transverse momentum distributions for each centrality bin were corrected for the geometrical acceptance of the detector, the efficiency of the tracking algorithm and the distortion due to binning and momentum resolution. The procedure for obtaining the correction factors was described in [6]. The largest contributions to the systematic uncertainty come from the overall tracking efficiency (5–10% uncertainty) and the reduction in overall acceptance due to malfunctioning

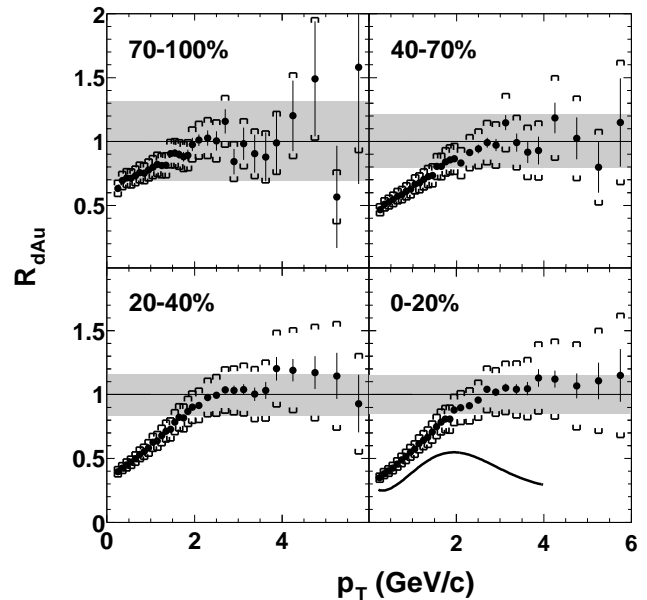


FIG. 3: Nuclear modification factor R_{dAu} as a function of p_T for four bins of centrality. For the most central bin, the spectral shape for central Au+Au data relative to $p+\bar{p}$ is shown for comparison. The shaded area shows the uncertainty in R_{dAu} due to the systematic uncertainty in $\langle N_{coll} \rangle$ and the UA1 scale error (90% C.L.). The brackets show the systematic uncertainty of the d+Au spectra measurement (90% C.L.).

channels in the silicon detectors (5% uncertainty). The corresponding corrections are centrality independent. The next largest correction is the p_T and centrality dependent momentum resolution and binning correction. The contamination by secondary particles and feeddown particles is small, due to the proximity of the tracking detectors to the collision vertex and the requirement for the reconstructed track to point back to the beam orbit to within 0.4 cm.

In Fig. 1, we present the invariant yield of charged hadrons as a function of transverse momentum, obtained by averaging the yields of positive and negative hadrons. Data are shown for four E_{Ring} centrality bins. The plot shows the evolution of overall yield and spectral shape with increasing collision centrality.

The centrality evolution of the spectra can be studied in detail in Fig. 2, where we compare our d+Au data to results from UA1 for $p+\bar{p}$ collisions at the same energy [17]. To account for the difference in acceptance between UA1 ($|\eta| < 2.5$) and PHOBOS, a correction function was determined using PYTHIA [18]. The quantity shown on the vertical axis in Fig. 2 is a direct measure of the

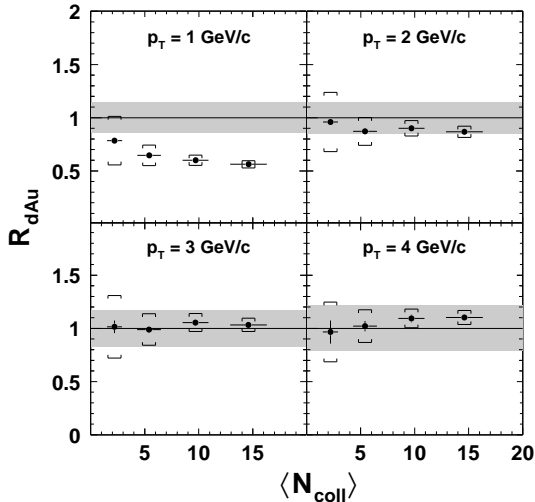


FIG. 4: Nuclear modification factor R_{dAu} as a function of centrality in four bins of transverse momentum. The brackets indicate the point-to-point systematic error, dominated by the uncertainty in the number of collisions for each centrality bin. The grey band shows the overall scale uncertainty at each p_T . Systematic errors are at 90% C.L.

modification of the spectral shape relative to $p + \bar{p}$ for each centrality bin in d+Au and is defined as follows: the fitted dN/dp_T distribution for each centrality bin is divided by the corrected fit to the UA1 $p + \bar{p}$ data [19]. The resulting distribution is normalized to unity at $p_T = 0.5$ GeV/c. Then the value of the normalized ratio at four values of p_T from 1 to 4 GeV/c is plotted against $dN/d\eta$ determined by integrating the hadron spectrum for each centrality bin. If there were no modification of the spectral shape relative to $p + \bar{p}$ collisions, the ratio would be flat at unity. This presentation of the data allows an investigation of the evolution of the spectral shape with increasing centrality, while eliminating the uncertainty associated with the determination of $\langle N_{coll} \rangle$. We observe that the relative yield for all p_T regions grows smoothly as a function of $dN/d\eta$, with the biggest increase relative to $p + \bar{p}$ observed at the largest p_T . For all p_T regions, the data extrapolate to the corrected $p + \bar{p}$ fit.

In Fig. 3 we present the nuclear modification factor R_{dAu} as a function of p_T for each centrality bin, defined as

$$R_{dAu} = \frac{\sigma_{p\bar{p}}^{inel}}{\langle N_{coll} \rangle} \frac{d^2 N_{dAu}/dp_T d\eta}{d^2 \sigma(\text{UA1})_{p\bar{p}}/dp_T d\eta}. \quad (1)$$

Consistent with our Glauber calculations, we used $\sigma_{pp}^{inel} = 41$ mb. A value of $R_{dAu} = 1$ corresponds to scaling of the yield as an incoherent superposition of nucleon-nucleon collisions. For all centrality bins, we observe a rapid rise of R_{dAu} from low p_T , leveling off at p_T of ≈ 2 GeV/c. For comparison, we also plot the results from central Au+Au collisions at the same energy [6] in the lower right panel of Fig. 3. The average number of collisions undergone by each participating nucleon in the central Au+Au collision is close to 6, similar to that of each nucleon from the deuteron in a central d+Au collision. For central Au+Au collisions, the ratio of the spectra to $p + \bar{p}$ rises rapidly up to $p_T \approx 2$ GeV/c, but falls far short of collision scaling at larger p_T , in striking contrast to the behavior for central d+Au collisions.

Predictions for the evolution of R_{dAu} from semi-peripheral collisions with $\langle N_{coll} \rangle \approx 6$ to central collisions were made in two qualitatively different models. Perturbative QCD calculations [20] predict an increase in the maximum value of R_{dAu} at $p_T \approx 3.5$ GeV/c by 15%. In contrast, a decrease in R_{dAu} by 25–30% over the same centrality range is predicted in a parton saturation model [8]. The centrality evolution of R_{dAu} is shown in Fig. 4, where the points were obtained from a fit to the p_T dependence of R_{dAu} in each centrality bin. Our data disfavor the prediction from the parton saturation model. This suggests that the observed suppression of high p_T hadrons in Au+Au collisions [3, 4, 5, 6] cannot be accounted for by initial state effects that should also be present in d+Au collisions.

This work was partially supported by US DoE grants DE-AC02-98CH10886, DE-FG02-93ER40802, DE-FC02-94ER40818, DE-FG02-94ER40865, DE-FG02-99ER41099, W-31-109-ENG-38, US NSF grants 9603486, 9722606, 0072204, Polish KBN grant 2-P03B-10323, and NSC of Taiwan contract NSC 89-2112-M-008-024.

-
- [1] J. W. Cronin *et al.*, Phys. Rev. **D11** (1975) 3105.
[2] For a recent review, see A. Accardi, arXiv:hep-ph/0212148.
[3] K. Adcox *et al.*, Phys. Rev. Lett. **88** (2002) 022301.
[4] K. Adcox *et al.*, arXiv:nucl-ex/0207009.
[5] C. Adler *et al.*, Phys. Rev. Lett. **89** (2002) 202301.

- [6] B. B. Back *et al.*, arXiv:nucl-ex/0302015, submitted to Phys. Lett. **B**.
[7] M. Gyulassy and M. Plümer, Phys. Lett. **243** (1990) 432.
[8] D. Kharzeev, E. Levin, L. McLerran, BNL preprint BNL-NT-02/22, arXiv:hep-ph/0210332.
[9] X. N. Wang, Phys. Rev. **C61** (2000) 064910.

- [10] S. S. Adler *et al.*, arXiv:nucl-ex/0306021
- [11] J. Adams *et al.*, arXiv:nucl-ex/0306024.
- [12] B. B. Back *et al.*, Nucl. Inst. Meth. **A499** (2003) 603.
- [13] C. Halliwell *et al.*, Phys. Rev. Lett. **39** (1977) 1499.
- [14] B. B. Back *et al.*, Phys. Rev. **C65** (2002), 061901.
- [15] M. Gyulassy and X. N. Wang, Comp. Phys. Comm. **83** (1994) 307. We used HIJING v1.383 with default parameters.
- [16] B. B. Back *et al.*, Phys. Rev. **C67** (2003) 021901.
- [17] C. Albajar *et al.*, Nucl. Phys. **B335**, (1990) 261.
- [18] T. Sjostrand, PYTHIA manual, Comp. Phys. Comm. **82** (1994) 74. We used PYTHIA 6.161.
- [19] The reference spectrum is well fitted by $\frac{1}{p_T} \frac{dN}{dp_T d\eta} = 50.9 \cdot (1+p_T/1.6)^{-11.143} \cdot \frac{p_T}{\sqrt{p_T^2+0.00545}}$, with p_T given in GeV/c.
- [20] I. Vitev, arXiv:nucl-th/0302002.